THE ASTRONOMICAL JOURNAL VOLUME 111, NUMBER 1 JANUARY 1996

A *ROSAT* SEARCH FOR CLUSTERS AROUND THREE POWERFUL RADIO GALAXIES AT REDSHIFTS $0.1 \lesssim z \lesssim 0.25$

CHRISTOPHER P. O'DEA
Space Telescope Science Institute,[1] Baltimore, Maryland 21218
Electronic mail: odea@stsci.edu

D. M. WORRALL
Harvard-Smithsonian Center for Astrophysics, Cambridge, Massachusetts 02138
Electronic mail: dmw@cfa.harvard.edu

STEFI A. BAUM
Space Telescope Science Institute, Baltimore, Maryland 21218
Electronic mail: sbaum@stsci.edu

CARLO STANGHELLINI
Istituto di Radioastronomia del CNR, Noto, Italy
Electronic mail: carlo@eloro.ira.noto.cnr.it

Received 1995 June 7; revised 1995 September 13

ABSTRACT

We report *ROSAT* PSPC observations of three powerful radio galaxies. We detect extended emission from the classical double radio galaxy 2053−201 ($z=0.1546$) with a 0.2–2 keV luminosity ($H_0=75$ km s^{-1} kpc^{-1}) of $L_x \sim 3\times10^{43}$ ergs s^{-1}, which overlaps the range of luminosities measured for Abell clusters at similar redshifts. We do not detect x-ray emission from the 2 GHz peaked spectrum (GPS) radio galaxies 1345+125 ($z=0.122$) and 2352+495 ($z=0.237$). The 3σ upper limits to the x-ray luminosity are about $L_x < 3\times10^{42}$ ergs s^{-1}, roughly an order of magnitude below the detection of 2053−201. These observations are consistent with the environments of GPS radio galaxies being poor clusters or groups, as indicated by optical imaging. The absence of strong nuclear x-ray emission from the AGN in the GPS galaxies suggests the GPS nuclei are either highly obscured or not intrinsically very powerful x-ray sources. Our x-ray upper limits for the GPS sources rule out two very promising candidates for confining the radio emission to its small subkpc physical size: a hot component of the ISM and a massive cooling flow. Any confining gas must be colder than $\sim10^6$ K. However, such gas has so far proved somewhat elusive, with existing radio data implying only modest column densities, insufficient to hide significant nuclear x-ray emission. Our x-ray limits allow hot-gas environments and emission components which are more consistent with measured lower-power (FR1) radio galaxies than with higher-power (FR2) sources. Thus, if GPS sources are young versions of powerful extended radio sources, then our results are consistent with them evolving into FR1 (or weaker) radio sources, i.e., their radio luminosity declines as the sources age.

1. INTRODUCTION

GHz peaked spectrum (GPS) and compact steep spectrum (CSS) radio galaxies (O'Dea *et al.* 1991; Fanti *et al.* 1990) make up significant fractions of the bright (cm wavelength selected) radio source population ($\sim$10% and $\sim$20%, respectively) but are not well understood. They are powerful but compact radio sources whose spectra are simple and convex, with peaks near 1 GHz and 100 MHz, respectively. The GPS sources are entirely contained within the extent of the narrow line region ($\lesssim$1 kpc), while the CSS sources are contained entirely within the host galaxy ($\lesssim$15 kpc).

There are two main hypotheses for the origin of GPS and CSS sources. (1) They could be radio galaxies in the early stages of their lives (Phillips & Mutel 1982; Carvalho 1985; Hodges & Mutel 1987; De Young 1993; Fanti *et al.* 1995; Readhead *et al.* 1995). In this scenario they might ultimately become large-scale powerful Fanaroff & Riley (1974) class 2 (FR2) radio sources or perhaps weaker (FR1) sources if they decline in luminosity as they age. (2) They could be confined to their present size scale via interaction with their ambient medium (e.g., van Breugel *et al.* 1984; Wilkinson *et al.* 1984; Fanti *et al.* 1990; Baum *et al.* 1990; O'Dea *et al.* 1991; Carvalho 1994). These "frustrated" sources never become large-scale doubles.

The presence of the GPS and CSS radio galaxies at redshifts $0.1 \lesssim z \lesssim 1$, and their absence at lower redshifts

[1]Operated by the Association of Universities for Research in Astronomy, Inc. under cooperative agreement with the National Aeronautics and Space Administration.

TABLE 1. Source list.

Source	1345+125	2053-201	2352+495
Type	GPS	Cl. Dbl.	GPS
z	0.122	0.1564	0.237
m(R_c)	15.2	16.1	17.8
M(R_c)	−23.5	−23.1	−22.6
D_{lum} (Mpc)	514	668	1050
scale (kpc/")	2.0	2.4	3.3
RA. (J2000.)	13H47M33.36S	20H56M04.25S	23H55M09.46S
DEC.	12°17'24.2"	−19°56'34.1"	49°50'08.2"
log $P_{1.4}$ (Watts Hz^{-1})	26.21	26.15	26.54
Linear Size (kpc)	0.25	72	0.50

Note. — A summary of global source properties. The references for the redshifts are Gilmore & Shaw (1986) - 1345+125; Caganoff (1990), Stickel & Kuhr (1994) - 2053-201; Pearson & Readhead (1988) - 2352+495. The Cousins R_c apparent and absolute magnitude for 1345+125 and 2352+495 are taken from O'Dea (1995, in preparation) and the values for 2053-201 are from this work using the transformation to Cousin R_c and the K correction from Frei & Gunn (1994). We adopt H_o = 75 km s^{-1}Mpc^{-1} and q_o = 0.1.

(O'Dea *et al.* 1991; Fanti *et al.* 1990),[2] suggest that their origin and evolution are tied to the dynamical evolution of galaxies and their cluster environments at these epochs. X-ray measurements probe the environments, and in this paper we present *ROSAT* PSPC observations of three powerful radio galaxies in the redshift range 0.1–0.25 (Table 1). The radio sources are well matched in radio power. However, the GPS radio sources (1345+125 and 2345+495—Shaw *et al.* 1992; Stanghellini *et al.* 1995; Wilkinson *et al.* 1994) are about two orders of magnitude smaller in physical size than the classical double (2053−201—this paper, see Fig. 4). The two GPS sources have radio morphologies which are similar to those of large-scale radio sources, i.e., they resemble small-scale versions of the larger double-lobed radio sources, rather than the core-jet type of radio morphology usually seen on the subkpc scale in powerful radio sources.

In Sec. 2 we present the *ROSAT* results for the three sources. In Sec. 3 we present VLA and NOT observations of 2053−201 and discuss the implications for its clustering environment. In Sec. 4, we discuss the implications of the *ROSAT* observations for the two GPS radio galaxies, including the clustering environment, confinement of the radio source, constraints on a possible cooling flow, obscuration of the central AGN, and the relationship to FR1 and FR2 radio galaxies.

2. X-RAY OBSERVATIONS AND RESULTS

We observed 1345+125, 2053−201, and 2352+495 in soft x rays with the *ROSAT* Position-Sensitive Proportional Counter (PSPC; Trümper 1983; Pfeffermann *et al.* 1987)

[2]Note that unlike the GPS galaxies which are found at moderate redshifts $0.1 \lesssim z \lesssim 1$, the GPS quasars tend to be found at high redshift $2 \lesssim z \lesssim 4$ (O'Dea 1990; Peterson *et al.* 1982).

TABLE 2. *ROSAT* PSPC x-ray observations.

Name	$N_{H_{Galactic}}$	Date	Exposure (s)
1345 + 125	1.1 × 10^{20}	1992 July 22	3,798
2053 − 201	5.5 × 10^{20}	1993 April 28 – May 9	11,289
2352 + 495	1.2 × 10^{21}	1992 August 7-8	2,810
		1992 December 24-26	13,317

Note. — The Galactic HI column densities are from Lockman (1991, private communication) and have 5% uncertainties.

during the pointed phase of the mission. The measurements, whose dates and exposure times given in Table 2, were taken in *ROSAT*'s normal "wobble" mode, and the data we received had already been corrected for instrumental effects and the motion of the satellite. Our further analysis of the data used the Post Reduction Off-line Software (PROS; Worrall *et al.* 1992) which runs in the IRAF environment, and the XSPEC spectral-fitting program.

For the two nondetections, two circular apertures were used, a 35″ radius aperture best suited for detecting a point source, and an extraction region corresponding to a radius of 200 kpc to place limits on extended emission. Background was taken locally from an annulus of radii 2–5 arcmin, excluding any sources detected by the Standard Analysis Software System (SASS, Gruber 1992). Only 2053−201 was detected. The spectral fits to the data are summarized in Table 3. The Raymond–Smith (Raymond & Smith 1977) thermal plasma gives a reasonable fit for a temperature of 3–4 keV and an absorbing column close to the Galactic value. However the abundance is poorly constrained. A power law can also fit the spectral data. However, the fact that the x-ray emission is extended suggests that it is predominantly thermal. The flux and luminosity, after correction for absorption in our Galaxy, are given in Table 4. 3σ upper limits for the two sources which were not detected were de-

TABLE 3. Spectral fits to 2053−201.

Name	Extraction radius arcsec	PSPC counts 0.17 to 2.4 keV	Flux Density at 1 keV μJy	Flux 0.2 − 2 keV 10^{-13} ergs cm^{-2} s^{-1}	Luminosity 0.2 − 2 keV 10^{42} ergs s^{-1}
1345+125	35	< 25.7	< 8.9 × 10^{-3}	< 0.58	< 1.7
1345+125	100	< 35.9		< 0.98	< 2.9
2053-201	120	492 ± 28	1.6 × 10^{-1}	6.6	32
2352+495	35	< 16.9	< 1.8 × 10^{-3}	< 0.12	< 1.4
2352+495	61	< 19.8		< 0.15	< 1.7

Note. — Upper limits are 3σ. For 2053−201 the spectral parameters used are the best fit values for a Raymond-Smith thermal model from Table 4. The abundance is not well constrained by the data so it was held fixed at 0.5 solar. The value of N(H) was consistent with the Galactic value and this was also held fixed. The derived temperature is ~ 4 keV. For the other two sources, the spectral parameters were fixed at values consistent with 2053-201, i.e., the abundance is 0.5 solar, the N(H) is the appropriate Galactic value and the temperature is fixed at 4.0 keV. The flux and flux density are corrected for absorption by the Galactic column density. The unabsorbed flux is given in the energy band 0.2 to 2 keV. For the two non-detections, 3σ upper limits are given for the counts, flux, flux density, and luminosity.

TABLE 4. X-ray fluxes and luminosities.

Abundance	kT	Raymond-Smith N(H)	χ^2_ν
	keV	10^{20} cm^{-2}	
0.0(+1.9, −0)	1.5(+8.8, −0.9)	7.4(+10.8, −2.4)	1.12
0.5 f	4.1(+16, −2.4)	5.3(+3.7, −1.5)	1.22
0.5 f	4.0(+13.6, −2)	5.46 f	1.17
	Γ	Powerlaw N(H)	χ^2_ν
		10^{20} cm^{-2}	
	2.3(+1.1, −0.7)	10.0(+14.0, −4.4)	1.02
	1.66(+0.25, −0.28)	5.46 f	1.13

Note. — A summary of the spectral fits to the PSPC data for 2053-201 using XSPEC. An 'f' indicates that the parameter was held fixed at that value for that fit. Errors shown in parentheses are one sigma for the appropriate number of free parameters. The R-S thermal plasma gives a reasonable fit for a temperature ~ 4 keV and an absorbing column close to the Galactic value. However, the abundance and temperature are poorly constrained. The power law can also fit the spectral data, though it requires a column density about a factor of two higher than the measured Galactic value. The results for PI channels 5 to 33 are given in the Table, however, the results did not change significantly when lower channels were included.

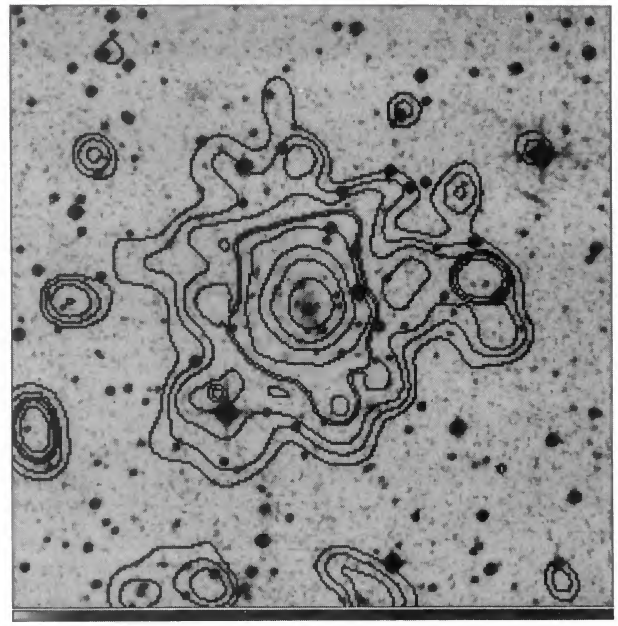

FIG. 2. Overlay of *ROSAT* image on optical field. Contours of the x-ray image from Fig. 1 are overlayed on the digitized image from "Quick *V*" survey of the Guide Stars Selection System Astrometric Support Program developed at STScI.

termined assuming spectral parameters similar to those fit for 2053−201, and are also given in Table 4.

The *ROSAT* image of 2053−201 is presented in Figs. 1 and 2. We detect the classical double with an x-ray luminosity of about 3×10^{43} ergs s^{-1} roughly independent of whether a Raymond–Smith or power-law model is used for the spectral fit. This luminosity is consistent with that of an Abell Cluster at this redshift ($\sim10^{43-45}$ ergs s^{-1}; e.g., Henry *et al.* 1982; Worrall *et al.* 1995), though it is towards the low end of the distribution.

To study the spatial extent of the x rays from 2053−201,

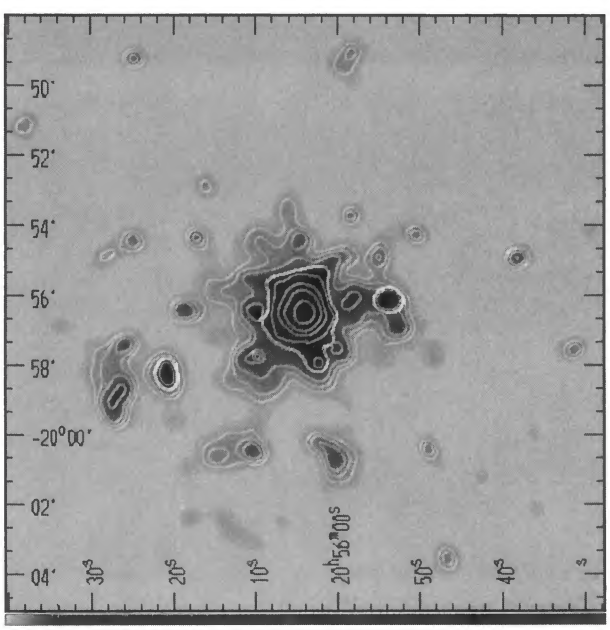

FIG. 1. The background subtracted and adaptively smoothed 0.2–2.3 keV PSPC x-ray image shows that the emission from 2053−201 is extended. The axes display J2000 equatorial coordinates. Contour levels, in units of 10^{-3} cts arcmin^{-2} s^{-1}, are 0.5, 0.8, 1.2, 1.9, 3.3, 5.0, 8.0, 12.0, 19.0. At the redshift (z=0.156) of the galaxy, 2′ corresponds to 290 kpc for H_0=75 km s^{-1} Mpc^{-1}, q_0=0.1.

we excluded intervals of high particle background, when the Master Veto Rate (MVRATE) was greater than 170. The resulting x-ray event file has 10 804 s of acceptable data. The background, which was determined locally from an annulus of radii 3′ and 5.′7, excluding regions contaminated by sources, was 1.14×10^{-3} counts arcmin^{-2} s^{-1} (0.2–2.3 keV). The resulting image was then adaptively smoothed, using the method of Worrall *et al.* (1995). The image was split into four separate images based on counting rate, with pixels not satisfying the selection condition set to zero. Each image was smoothed with a Gaussian of a particular sigma, so that areas of lowest counting rate were smoothed the most, and the resulting images were added. The divisions (in units of cts arcmin^{-2} s^{-1}), were $\geqslant3.1\times10^{-3}$, from $\geqslant1.5\times10^{-3}$ to $<3.1\times10^{-3}$, from $\geqslant4.0\times10^{-4}$ to $<1.5\times10^{-3}$, and $<4.0\times10^{-4}$, and the sigmas of the Gaussians were 24″, 31″, 38″, and 114″, respectively. The resulting image, superimposed with contours, is shown in Fig. 1.

In order to characterize the extent of the emission, we have fit models to the radial profile, using the method of Worrall & Birkinshaw (1994). We used only data for the energy range 0.2–1.9 keV, where the PSPC point response is well modeled; the profile contains 548±55 net counts. Best-fit parameters were determined for a fit of the background-subtracted radial profile to an unresolved component, a β model which is appropriate for gas in hydrostatic equilibrium (Cavaliere & Fusco-Femiano 1978; Sarazin 1986), and a combination of an unresolved component and a β model. An unresolved component alone gives an unacceptable fit (χ^2=988 for 41 degrees of freedom). The best fit to an hydrostatic β model is good (Fig. 3) and indicates hot gas of cluster dimension. However, the value for β of 0.5 is a little low for cluster-scale emission (see, e.g., Sarazin 1986). When a more typical value of β=2/3 is used, the addition of

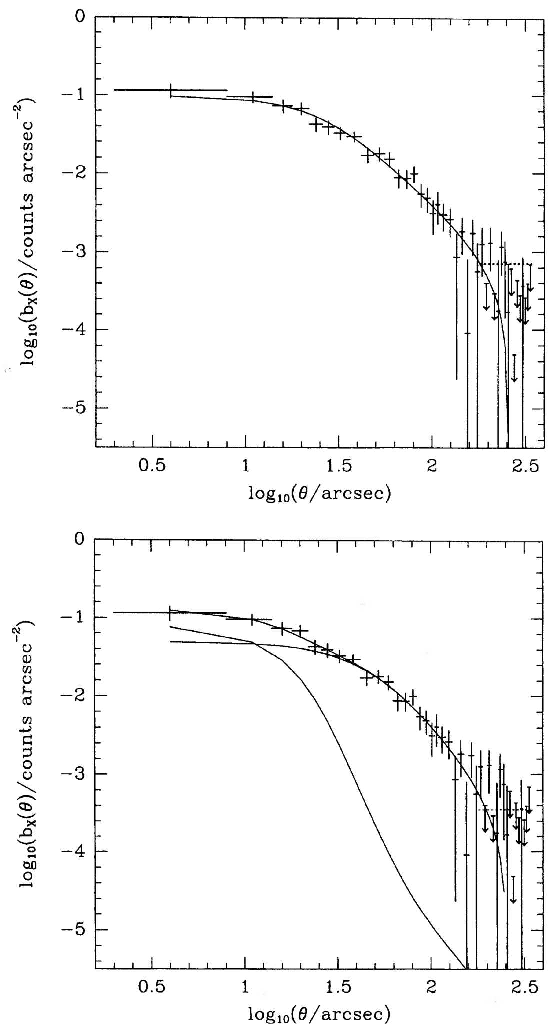

FIG. 3. Background-subtracted x-ray radial profile (0.2–1.9 keV) for 2053−201. The top plot shows the data with the best-fit β model (β=0.5, θ_{cx}= 16″; χ^2=29.5 for 40 degrees of freedom). A larger β more common for clusters is possible, but significantly (F test) prefers an additional unresolved component. The bottom plot is for β=2/3, θ_{cx}=45″, ~13% of net counts in an unresolved component; χ^2=27.0 for 39 dof. The dotted curve in each plot shows the contribution, taken into account in the fitting, of the model to the background annulus.

unresolved emission (~13% of the net counts) is a significant improvement according to an F test (F=17; <0.1% probability of happening by chance). This weak unresolved emission may be thermal, or it may be related to nonthermal emission from the radio core, a possibility discussed for nearby low-power radio galaxies by Worrall & Birkinshaw (1994).

3. THE CLASSICAL DOUBLE 2053−201

3.1 Optical and Radio Results

We obtained VLA[3] (Napier *et al.* 1983) images of 2053−201 in the A configuration at 90, 20, and 6 cm. The results

[3]The VLA is operated by the U.S. National Radio Astronomy Observatory which is operated by Associated Universities, Inc., under cooperative agreement with the National Science Foundation.

TABLE 5. VLA observations of 2053−201.

frequency MHz	clean beam	rms noise mJy	total flux density NE lobe Jy	SW lobe Jy	core mJy
302	8.6 × 5.6 PA = −18.1	5	3.86	3.85	...
333	7.7 × 4.9 PA = −18.3	5	3.45	3.54	...
1335	2.0 × 1.3 PA = −18.5	0.8	1.42	1.47	< 5
1665	1.7 × 1.1 PA = −17.0	0.8	1.18	1.17	< 5
4535	2.0 × 2.0 PA = 0.0	1	0.204	0.206	13
4985	2.0 × 2.0 PA = 0.0	1	0.150	0.195	10

Note. — The flux densities of the lobes have uncertainties of ~ 5% except at 6 cm, where we are systematically underestimating the flux density due to the lack of short uv spacings.

are summarized in Table 5 and contour plots of the images are shown in Fig. 4. The images show a classical double morphology with some rotation symmetry possibly due to precession of the radio jet. A weak core ~10 mJy is seen in the 6 cm image.

We obtained optical i and r band (in the Wade *et al.* 1979 system) images with the Nordic Optical Telescope. The data were reduced as described by Stanghellini *et al.* (1993). The optical magnitudes are $m(r)=16.4$, and $m(i)=15.9$. We transform to Cousins R_c and obtain an absolute magnitude of $M(R_c)\simeq-23.1$, using transformations and K corrections from Frei & Gunn (1994). The i-band image (Fig. 5) shows that the radio galaxy has a large envelope and is surrounded by many fainter galaxies. At present we know the redshift of only the radio galaxy. If the nearby (in projection) galaxies are at a similar redshift, then the radio galaxy is probably the dominant galaxy in a cluster.

3.2 Implications for the Clustering Environment

We find that (1) the x-ray emission is extended, (2) it is consistent with a Raymond–Smith model for a thermal gas, (3) the x-ray luminosity is consistent with that of typical Abell clusters. Based on our optical imaging, the host galaxy is likely to be the dominant galaxy in a cluster at a redshift of 0.156. Thus our results are consistent with us having detected x-ray emission from a cluster of galaxies at a redshift of 0.156 surrounding the radio galaxy. Redshifts of the possible cluster members are clearly needed.

Using our best-fit spectral model for the x-ray emission in 2053−201 we estimate the x-ray luminosity in the 2–10 keV band and convert to a Hubble constant of 50 km s^{-1} Mpc^{-1} in order to compare with the results of David *et al.* (1993). We estimate a 2–10 keV luminosity ~6.6×10^{43} ergs s^{-1}. Given our temperature estimate of 4 keV, the x-ray luminosity is in good agreement with the relationship between temperature and luminosity found by David *et al.*

The optical and x-ray evidence that 2053−201 is in a moderately rich cluster at z=0.156 is consistent with the finding that powerful (Fanaroff and Riley class 2, classical double) radio galaxies tend to be found in rich cluster environments at redshifts ≳0.1 (e.g., Hill & Lilly 1991; Yates *et al.* 1989; Smith *et al.* 1995).

We note that the large-scale optical envelope of the galaxy (Fig. 5) and the x-ray emission on the inner roughly 2′ scale

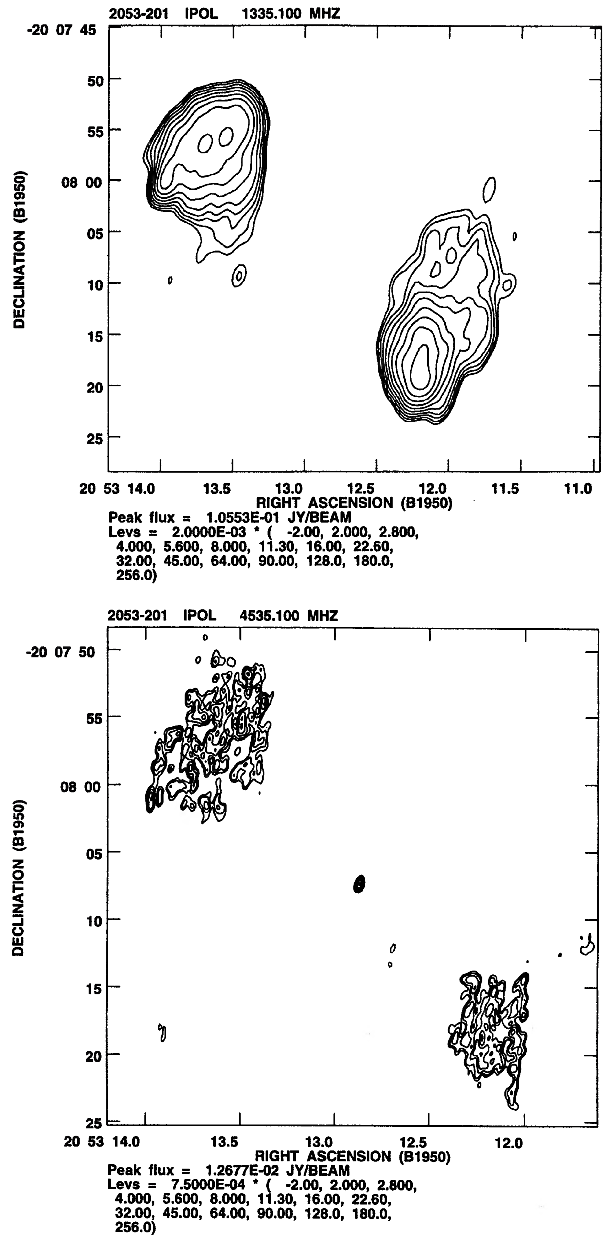

FIG. 4. 2053−201. On the top is the VLA A-array image at 1335 MHz. On the bottom is the VLA A-array image at 4535 MHz. Parameters of the images are given in Table 5. The 4535 MHz observations resolve out much of the flux density of the lobes. However, they do detect the radio core. The radio position of the nucleus is (B1950.0) R.A.=20 53 12.870, DEC =−20 08 7.40 with an uncertainty of 0.1 arcsec.

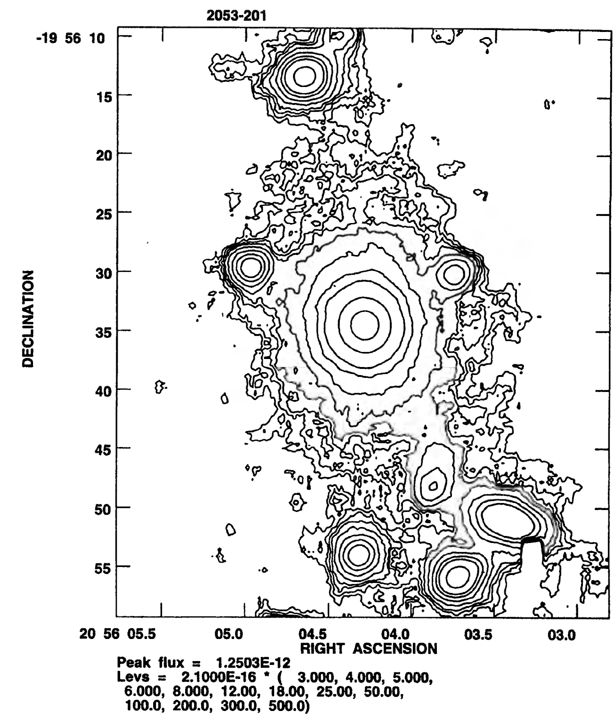

FIG. 5. 2053−201. Nordic Optical Telescope image in the *i* band. Units are ergs s^{-1} cm^{-2} $arcsec^{-2}$. Coordinates are equinox J2000.

(Figs. 1 and 2) are oriented in the same (north-south) direction. This is consistent with the tendancy for first ranked cluster galaxies to be aligned with the parent cluster (e.g., West 1994; de Theije *et al.* 1995).

4. THE TWO GPS GALAXIES 1345+125 AND 2352+495

4.1 Introduction

1345+125 and 2352+495 are two of the lowest redshift GPS radio galaxies currently known (O'Dea *et al.* 1991) and so were good candidates for pioneering *ROSAT* observations of the class. Both of these objects show radio morphology which is different from the "core-jet" structure found in typical powerful compact radio-loud AGN. The radio source in 1345+125 (Stanghellini *et al.* 1995, see also Shaw *et al.* 1992) is oriented roughly north-south, perpendicular to the direction of the merging Seyfert nucleus (see Gilmore & Shaw 1986). The location of the radio nucleus is unknown pending observations at another wavelength, but it is probably the most compact component (the most northerly of the three knots in the jet). The radio source shows a narrow winding jet ending in a diffuse lobe to the south. To the north of the probable core there are only a couple of faint components. If the emission on the northern side of the core is very diffuse it would be hard to detect in these radio observations.

2352+495 (Wilkinson *et al.* 1994; Readhead *et al.* 1995) shows a triple structure, with a bright core and two lobes to the NW and SE, with slight "*S*" symmetry. The type of two-sided symmetric structure seen in 2352+495 and to a lesser extent in 1345+125 has led to them being called "compact symmetric objects" (Conway *et al.* 1994; Wilkinson *et al.* 1994). Although these objects resemble large-scale radio sources in their morphology, they are subkpc in size. If these sources are small because they are tightly confined by dense gas in their environment, we may see clues in the x-ray emission from the host galaxy or the surrounding cluster.

4.2 Implications for the Clustering Environment

In contrast to the classical double 2052−201, the two GPS galaxies are not detected in either the point source extraction region or the "cluster" extraction region. The 3σ upper limit to the x-ray luminosity ($L_x < 3\times10^{42}$ ergs s^{-1};

Table 4) is too low to be consistent with emission from a typical Abell cluster but is consistent with the x-ray luminosity of early-type galaxies ($L_x \sim 10^{39-41}$ ergs s^{-1}, Forman *et al.* 1985) and of groups or poor clusters of galaxies with central dominant galaxies ($L_x \sim 10^{41-43}$ ergs s^{-1}, e.g., Mulchaey *et al.* 1995; Dell'Antonio *et al.* 1994; Kriss *et al.* 1983). The optical fields around 1345+125 (Stanghellini *et al.* 1993; O'Dea *et al.*, in preparation) and 2352+495 (O'Dea *et al.* 1990) are consistent with such an environment, and optical imaging of other GPS galaxies reveals that they too tend to be the dominant galaxy in a group or poor cluster (Stanghellini *et al.* 1993; O'Dea *et al.* 1990). In poor environments, an encounter with a gas-rich galaxy is possible, leading to accretion of the gas needed to (1) trigger the nuclear activity, (2) confine and depolarize the radio source. In fact 1345+125 does appear to be merging with a gas-rich Seyfert galaxy (e.g., Gilmore & Shaw 1986; Heckman *et al.* 1986; Hutchings 1987; Sanders *et al.* 1988; Baum *et al.* 1988; Smith & Heckman 1989; Mirabel *et al.* 1989; Stanghellini *et al.* 1993).

4.3 Confinement of the Radio Sources

Here we examine whether the hot component of the ISM of the host galaxies can thermally confine the radio sources. The minimum pressures in the radio source "lobes" are $P \sim 10^{-6}$ dynes cm^{-2} (using standard assumptions, Stanghellini *et al.* 1995; Readhead *et al.* 1995). In order to calculate constraints on the pressure of the hot ISM, we assume an isothermal β model for the gas, with β=2/3 and a core radius of 1 kpc (compact compared with typical galaxy and group gas but large enough to encompass the radio structures comfortably), an abundance of 50% cosmic, an absorbing column equal to the Galactic value, and adopt a Raymond–Smith emissivity for the gas. Our *ROSAT* observations then give upper limits to the central gas density of about 1 cm^{-3} over the range in gas temperature 0.1–7 keV (Fig. 6). This is consistent with the pressure of order 10^{-9} dynes cm^{-2} estimated for the narrow line clouds by Readhead *et al.* (1995), and is about two to three orders of magnitude too low to statically confine the radio source. (A larger core radius and smaller β, more typical of galaxy and group gas, would increase the discrepancy still further.)

If the source advance is not slowed by collisions with clouds (Carvalho 1994; De Young 1991; Balsara 1991) and the lobes are in ram pressure balance with the hot ISM, then the advance speed (v_a) is given by

$$v_a \gtrsim 0.026c\left(\frac{P_l}{10^{-6}}\right)^{1/2}\left(\frac{n}{1}\right)^{-1/2}, \qquad (1)$$

where P_l is the lobe pressure in dynes cm^{-2} and n is the ambient density in cm^{-3} (cf. Readhead *et al.* 1995).

A complementary approach has been taken by Fanti *et al.* 1995) who presented models for the growth of GPS and CSS sources into large-scale powerful radio sources (cf. Carvalho 1985; De Young 1993; Readhead *et al.* 1995). Given the observed radio luminosity they estimate the minimum momentum flux in the jets. They estimate the properties of the ISM of the host galaxy which would be required to limit the size

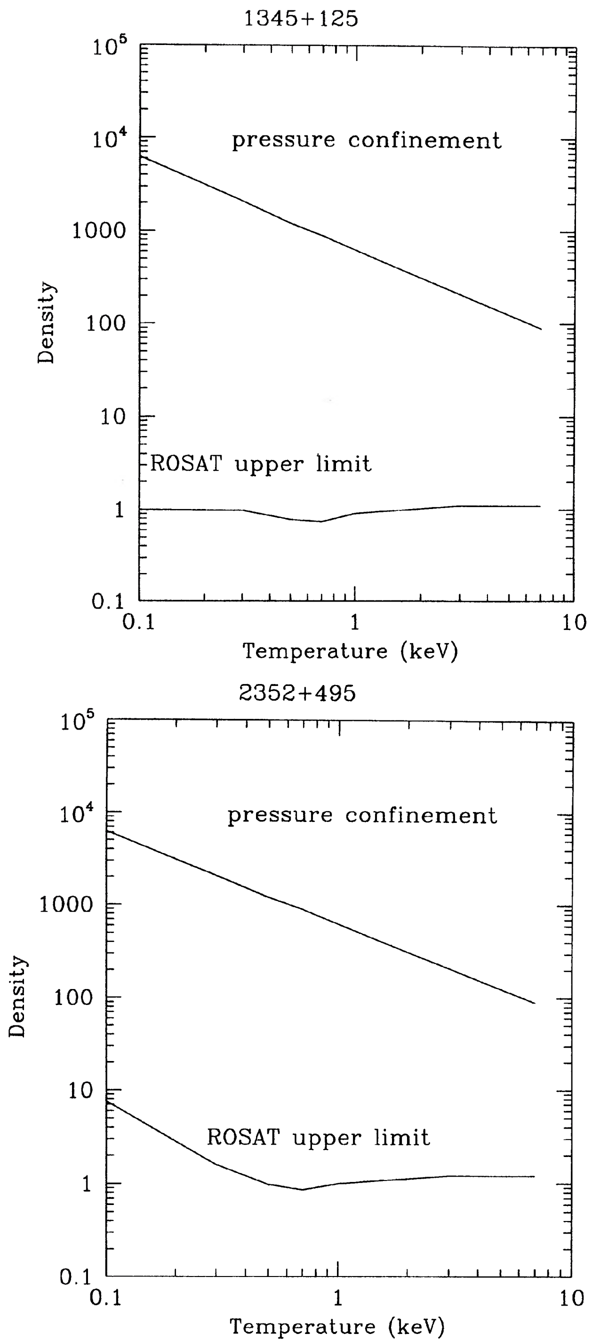

FIG. 6. Constraints on the central density as a function of temperature. The lower curve is the upper limit on the central density from our *ROSAT* observations assuming a β model with core radius 1 kpc. The upper curve is the density required to pressure confine the compact radio source with $P=10^{-6}$ dynes cm^{-2}.

of the radio source to 15 kpc after 2×10^7 yr. They estimated values for central density and core radius of the hot ISM predict x-ray luminosities in the 0.2–2 keV band of between 0.5 and 3×10^{44} ergs s^{-1} for jet powers in the range 1–2.4$\times10^{44}$ ergs s^{-1}. This is one to two orders of magnitude higher than our upper limits.

If our results can be generalized, our observations suggest that the hot component of the ISM in GPS and CSS galaxies cannot be responsible for confining the radio sources. This suggests that the radio sources are not confined and might expand to become large-scale radio sources (e.g., Phillips & Mutel 1982; Carvalho 1995; Hodges & Mutel 1987; De Young 1993; Fanti *et al.* 1995; Readhead *et al.* 1995). Alternately, the radio sources could be confined if they are confined by another component of the ISM, e.g., dense, cold gas.

4.4 Constraints on Cooling Flows in GPS Sources

One possible source of the high-pressure gas needed to confine the radio source is a large cooling flow. We can use the upper limit on the x-ray luminosity to place an upper limit on the mass accretion rate from a cooling flow around the GPS radio galaxies.

The mass accretion rate $\dot{m}$ is given by (e.g., Fabian 1994)

$$\dot{m} \simeq \frac{2}{5} L_{\rm cool} \frac{\mu m_H}{kT}, \qquad (2)$$

where $L_{\rm cool}$ is the x-ray luminosity of the gas whose cooling time is less than the Hubble time, $\mu=0.6$ is the mean molecular weight, m_H is the mass of a hydrogen atom, k is the Boltzmann constant, and T is the temperature of the x-ray emitting gas. We adopt a temperature of 4 keV which is consistent with our results on 2053−201 and is typical of clusters in general (David *et al.* 1993). We adopt an upper limit for $L_{\rm cool}$ equal to our 3σ upper limit on the total x-ray luminosity of $L_{\rm cool}<3\times10^{42}$ ergs s^{-1}, which is conservative since $L_{\rm cool}$ is usually 10% of the total x-ray emission. We derive an upper limit to the mass accretion rate of $\dot{m}<3$ $\mathscr{M}_\odot$ yr^{-1}. Thus our results are consistent with the hypothesis that GPS galaxies are not in (or are confined by) massive cooling flows.

4.5 Comparison with OQ 208

Zhang & Marscher (1994) report the *ROSAT* detection of OQ 208 (1404+286) which is a broad line radio galaxy at $z=0.077$ (e.g., Marziani *et al.* 1993). The GPS radio source is a powerful ($\log_{10}$ ($P_{1.4}$/W Hz^{-1})$\simeq$24.9) compact double with a separation of 10 pc (Stanghellini *et al.* 1995). Zhang & Marscher fit a single power law to the OQ 208 data and derive a flux density at 1 keV of 0.032±0.016 μJy, an x-ray power-law spectral index of $\alpha_x=1.97\pm0.73$, and a flux of $\sim8.0\times10^{-14}$ ergs cm^{-2} s^{-1} (0.3–2.5 keV). Adopting this flux, and ignoring the differences in the energy band, we estimate an x-ray luminosity of $\sim10^{42}$ ergs s^{-1} which is a factor of 3 less than our 3σ upper limits for 1345+125 and 2352+495. Thus, the data are consistent with OQ 208, 1345 +125, and 2352+495 all having similar soft x-ray luminosities of order 10^{42} ergs s^{-1}. Zhang & Marscher also report evidence for an *intrinsic* column density of hydrogen of N(H)$\simeq1.7\times10^{21}$ cm^{-2} in OQ 208.

4.6 Are the AGN in GPS Radio Galaxies Obscured?

The lack of a detection of the central engine in x rays in the GPS sources could be due to either (1) the AGN are intrinsically weak in x rays or (2) the soft x rays to which these *ROSAT* observations are sensitive are obscured by large columns of cool gas surrounding the nuclei. In this section we discuss the evidence for such large columns of gas and their possible effect on our results.

Elvis *et al.* (1994) report *ROSAT* observations of six high redshift ($2.8\lesssim z\lesssim3.8$) quasars three of which showed evidence for low-energy excess absorption. The six sources include three which are known to have GPS. Both of the GPS sources with good *ROSAT* data show evidence for excess absorption. The third source to show the absorption has a poorly determined radio spectrum and thus it is not known whether it has a GPS. The excess column densities correspond to N(H)$\sim10^{22}$ cm^{-2}. Elvis *et al.* suggest that the results show that high-z quasars are more likely to show absorption than low-z quasars. They suggest the following possible explanations (1) Intervening: damped Lα systems (2) Intrinsic: cooling flows. If it turns out to be true that GPS quasars are more likely to show the absorption than non-GPS quasars, this would favor an intrinsic explanation, e.g., a cooling flow as suggested by Elvis *et al.* (although we have shown that at least these two low redshift GPS galaxies are not in large cooling flows). Alternately, the absorption might be associated with ambient cold gas which confines the radio source (O'Dea *et al.* 1991).

The evidence for intrinsic x-ray absorption in GPS quasars (Elvis *et al.* 1994) and in the BLRG OQ 208 (Zhang & Marscher 1994) suggests that GPS radio sources may have significant absorbing columns between us and their nuclei. At this time it is not clear what the relationship between the GPS galaxies and quasars is. If the GPS galaxies have similar central engines to the GPS quasars, the obscuring columns between us and the central engine should be much higher in the galaxies than in the quasars (since we see broad optical emission lines in the quasars but not in the galaxies).

O'Dea *et al.* (1994) and Heckman *et al.* (1994) report a study of the *IRAS* emission from samples of GPS and compact steep spectrum (CSS) radio sources. 1345+125 is one of the few GPS galaxies detected individually with *IRAS*, with a 60 μm luminosity of 3.7×10^{45} ergs s^{-1}. In addition, the median values for the coadded data of the sample as a whole suggest that the GPS and CSS galaxies have typical mid-far-IR luminosities $\sim10^{12}$ $L_\odot$ ($\sim4\times10^{45}$ ergs s^{-1}). It is not clear whether the IR emission is powered mainly by a starburst associated with the nuclear activity or by nuclear continuum from the UV to x rays.

In Table 6 we give the 0.2–2.0 keV nuclear luminosities which would be consistent with our upper limit on the PSPC counts as a function of the intrinsic absorbing column density. We adopt a power-law energy index of 1.0 for the nuclear emission, and also include the effects of the measured Galactic column density. Intrinsic absorbing columns of a few $\times10^{22}$ cm^{-2} are sufficient to hide x-ray luminosities of between 10^{43} and 10^{44} ergs s^{-1}. This is still less than the amount of reprocessed luminosity observed in the IR. Additional observations are needed to determine whether there is indeed a luminous hidden nucleus (e.g., higher-energy x-ray observations).

Is there evidence for sufficient column densities of cold gas in these two sources to hide a bright x-ray nucleus? 1345 +125 appears to be merging with a gas-rich Seyfert galaxy

TABLE 6. Constraints on obscured nuclear x-ray luminosity.

$N_{H_{Intrinsic}}$	Maximum Permitted Luminosity 10^{42} ergs s^{-1} 1345+125	2352+495
0.0	2.3	4.3
1×10^{20}	2.8	4.4
5×10^{20}	4.1	4.8
1×10^{21}	5.1	5.2
5×10^{21}	11	8.7
1×10^{22}	21	15
2×10^{22}	51	31
3×10^{22}	106	57
4×10^{22}	199	97
5×10^{22}	351	158
7×10^{22}	978.	377
1×10^{23}	3828	1195

Note. — We adopt a power-law energy index of 1.0 and include the measured Galactic N(H) column density.

(e.g., Gilmore & Shaw 1986; Baum *et al.* 1988; Mirabel *et al.* 1989; Stanghellini *et al.* 1993). The presence of substantial amounts of gas in this system is supported by (1) the large Infrared flux densities, 1345+125 is an Ultra Luminous Infrared Galaxy (e.g., Golombek *et al.* 1988) and (2) the detection of CO in emission (Mirabel *et al.* 1989) and H I in absorption (Mirabel 1989). Assuming a uniform covering factor of the H I over the radio source, the H I column density is $N(\mathrm{H})\cong6.2\times10^{18}T_s$ cm^{-2}, where T_s is the spin temperature (Mirabel 1989). For values of spin temperature of 100–1000 K, the column density is $\sim6\times10^{20-21}$ cm^{-2}. The ^{12}CO(1$\rightarrow$0) flux integral is $W_{\mathrm{CO}}\cong0.75$ K km s^{-1} (Mirabel *et al.* 1989). Adopting the Galactic conversion between CO flux integral and molecular hydrogen column density $N(\mathrm{H}_2)\cong2.8\times10^{20}W_{\mathrm{CO}}$ cm^{-2} (e.g., Bloemen *et al.* 1986; Scoville & Sanders 1987; Young & Scoville 1991) and assuming a unity covering factor over the beam of the NRAO 12 m gives a column density of $N(\mathrm{H}_2)\sim2.1\times10^{20}$ cm^{-2}. If the CO solid angle (Ω_{CO}) is less than the solid angle of the NRAO 12 m beam (Ω_{12-m}) then the upper limit on the column density is increased by the factor $\Omega_{12-m}/\Omega_{\mathrm{CO}}$ which is potentially very large.

At the current time there is no direct evidence for significant amounts of cold gas in 2352+495. Readhead *et al.* (1995, and private communication) report upper limits of 0.05 and 0.10 on the optical depth from H I and CO, respectively. The column density of atomic hydrogen is given by

$$N(\mathrm{H})\simeq1.94\times10^{18}T_s\tau_o\Delta V, \tag{3}$$

where T_s is the spin temperature, τ_o is the peak optical depth in the line, and ΔV is the FWHM of the Gaussian line profile (e.g., Kerr 1968; Verschuur 1974). If we adopt guesses for the spin temperature of 100–1000 and for the velocity FWHM of 500 km s^{-1}, we obtain limits on the column density of $N(\mathrm{H})<5\times10^{21-22}$ cm^{-2}. The upper limit on the CO is difficult to interpret since the nonthermal radio continuum may increase the excitation temperature of the CO, greatly reducing the optical depths (Maloney *et al.* 1994).

At the present time there is no *direct* evidence for column densities of gas which are sufficient to obscure an x-ray bright nucleus. Further searches for gas on the parsec scale in these two GPS sources are needed to resolve this question.

4.7 Comparison with FR1 and FR2 Radio Galaxies

The *Einstein Observatory* established the presence of x-ray emission in FR1 and FR2 radio galaxies (Feigelson & Berg 1983; Fabbiano *et al.* 1984). *ROSAT*'s superior spatial resolution and sensitivity has led to improved knowledge, particularly for nearby low-power (FR1) radio sources. FR2 sources for which there are x-ray measurements tend to give luminosities which are much higher than the upper limits for the GPS sources (Fabbiano *et al.* 1984; Arnaud *et al.* 1984; Worrall *et al.* 1994; Crawford & Fabian 1993, 1995).

ROSAT measurements of a complete sample of FR1 radio galaxies selected from the "B2 bright sample" (Ulrich 1989) with $z<0.06$ and $24.0\leqslant\log P_{1.4}\leqslant25.2$ (W Hz^{-1}) reveals that the x-ray emission in most of the sources is dominated by an extended component from thermal gas of at most "group" rather than cluster size and strength (Morganti *et al.* 1988; Feretti *et al.* 1995; Worrall & Birkinshaw 1994, and work in preparation). The typical gaseous environment of the B2 bright sample galaxies is not rich, and only 1 of 15 lies in an Abell cluster.[4] Although a weaker unresolved component of x-ray emission is also normally measured, results are currently inconclusive as to a thermal or nuclear origin for this. Typical (0.2–2 keV) total luminosities are of order 5×10^{41} ergs/s ($H_0=75$ km s^{-1} Mpc^{-1}), which is consistent with the upper limits for the two GPS sources reported here. GPS sources (although at least an order of magnitude more radio luminous than typical FR1 sources) could therefore live in environments typical of FR1s (or at least the subset of local FR1 radio galaxies in poor environments). Thus, our results are consistent with the hypothesis that GPS sources are in an early stage of development and decline in radio luminosity to become FR1 radio sources as they age.

5. SUMMARY

We report *ROSAT* PSPC observations of three powerful radio galaxies. Images from the VLA and Nordic Optical Telescope show that 2053−201 is a classical double radio galaxy associated with what is probably the dominant galaxy in a cluster at a redshift of $z=0.156$. In our *ROSAT* observations, we detect extended emission from the classical double radio galaxy 2053−201 with a luminosity of $L_x\sim3\times10^{43}$ ergs s^{-1}. The fits to the spatial profile are consistent with about 13% of the x-ray flux in an unresolved component. The x-ray luminosity of the extended component is consistent with the expected emission from an Abell cluster at these redshifts (e.g., Henry *et al.* 1982) and also with previous detections of 3CR FR2 radio galaxies (Fabbiano *et al.* 1984; Feigelson & Berg 1983).

We do not detect any x-ray emission from the two GHz peaked spectrum (GPS) radio galaxies 1345+125 and 2352

[4]The clustering environments of low redshift FR1 sources covers the range from rich to poor (e.g., Prestage & Peacock 1988).

+495. The 3σ upper limits to the x-ray luminosity are on the order of $L_x < 3\times10^{42}$ ergs s^{-1} and are about an order of magnitude below the detection of 2053−201. These upper limits are too low to be consistent with emission from a typical Abell cluster, but could be consistent with the x-ray luminosity of poor clusters with central dominant galaxies (Kriss *et al.* 1983) or from groups of galaxies (Dell'Antonio *et al.* 1994; Mulchaey *et al.* 1995).

The absence of strong nuclear x-ray emission from the AGN in the GPS galaxies suggests either the GPS nuclei are highly obscured or are not intrinsically very powerful x-ray sources.

Our x-ray upper limits for the GPS sources rule out two very promising candidates for confining the radio emission to its small subkpc physical size: a hot component of the ISM, and a massive cooling flow. Any confining gas must be colder than $\sim 10^6$ K, possibly acquired in a merger. However, such gas has so far proved somewhat elusive, with existing radio data implying only modest column densities, insufficient to hide significant nuclear x-ray emission.

Our x-ray limits allow hot-gas environments and emission components which are more consistent with measured lower-power (FR1) radio galaxies than with higher-power (FR2) sources. However, the high radio luminosities of the GPS galaxies are comparable to those of the FR2s rather than the FR1s. Thus, if GPS sources are young versions of powerful extended radio sources, then our results are consistent with them evolving into FR1 (or weaker) radio sources, i.e., their radio luminosity declines as the source age.

This research was partially supported by NASA Grant No. NAG5-2158 from the *ROSAT* Guest Observer Program. We are grateful to Diane Gilmore for her expert help with the *ROSAT* data reduction, to Bob Mutel for his enthusiasm and encouragement, and to Mark Birkinshaw and Tim Heckman for comments on the manuscript. We thank the anonymous referee for helpful comments. We thank Al Marscher and Yun Fei Zhang for sharing their results on OQ 208 in advance of publication, Tony Readhead and Greg Taylor for sharing their results on 2352+495 in advance of publication, and Jay Lockman for sharing his results on Galactic H I column density in advance of publication. DMW acknowledges support from NASA Contract No. NAS8-39073.

REFERENCES

Allen, S. A., & Fabian, A. C. 1992, MNRAS, 258, 29p
Arnaud, K. A., Fabian, A. C., Eales, S. A., Jones, C., & Forman, W. 1984, MNRAS 211, 981
Balsara, D. S. 1991, Ph.D. thesis, University of Illinois
Baum, S. A., O'Dea, C. P., Murphy, D. W., & de Bruyn, A. G. 1990, A&A, 232, 19
Birkinshaw, M., & Worrall, D. M. 1993, ApJ, 412, 568
Bloemen, J. B. G. M., *et al.* 1986, A&A, 154, 25
Bloom, S. D., & Marscher, A. P. 1991, ApJ, 366, 16
Caganoff, S. 1989, Ph.D. thesis, Australia National University
Carvalho, J. C. 1985, MNRAS, 215, 463
Carvalho, J. C. 1994, A&A, 292, 392
Cavaliere, A., & Fusco-Femiano, R. 1978, A&A, 70, 677
Conway, J. E., Myers, S. T., Pearson, T. J., Readhead, A. C. S., Unwin, S. C., & Xu, W. 1994, ApJ, 425, 568
Crawford, C. S., & Fabian, A. C. 1993, MNRAS, 260, L15
Crawford, C. S., & Fabian, A. C. 1995, MNRAS, 273, 827
David, L. P., Slyz, A., Jones, C., Forman, W., Vrtilek, S. D., & Arnaud, K. A. 1993, ApJ, 412, 479
Dell'Antonio, I. P., Geller, M. J., & Fabricant, D. G. 1994, AJ, 107, 427
de Theije, P. A. M., Katgert, P., & van Kampen, E. 1995, MNRAS, 273, 30
De Young, D. S. 1991, ApJ, 371, 69
De Young, D. S. 1993, ApJ, 402, 95
Elvis, M., Fiore, F., Wilkes, B., McDowell, J., & Bechtold, J. 1994, ApJ, 422, 60
Fabbiano, G., Miller, L., Trinchieri, G., Longair, M., & Elvis, M. 1984, ApJ, 277, 115
Fabian, A. C. 1994, ARA&A, 32, 277
Fanaroff, B., & Riley, J. 1974, MNRAS, 167, 31p
Fanti, R., Fanti, C., Schilizzi, R. T., Spencer, R. E., Rendong, N., Parma, P., van Breugel, W. J. M., & Venturi, T. 1990, A&A, 231, 333
Fanti, C., Fanti, R., Dallacasa, D., Schilizzi, R. T., Spencer, R. E., & Stanghellini, C. 1995, A&A (in press).
Feigelson, E. D., & Berg, C. J. 1983, ApJ, 269, 400
Feretti, L., Fanti, R., Parma, P., Massaglia, S., Trussoni, E., & Brinkman, W. 1995, A&A, 298, 699
Frei, Z., & Gunn, J. E. 1994, AJ, 108, 1476
Gilmore, G. & Shaw, M. A. 1986, Nature, 321, 750
Golombek, D., Miley, G. K., & Neugebauer, G. 1988, AJ, 95, 26
Gruber, R. 1992, in Data Analysis in Astronomy IV, edited by V. Di Gesu *et al.* (Plenum, New York), p. 153.
Heckman, T. M., Smith, E. P., Baum, S. A., van Breugel, W. J. M., Miley, G. K., Illingworth, G. D., Bothun, G. D., & Balick, B. 1986, ApJ, 311, 526
Heckman, T. M., O'Dea, C. P., Baum, S. A., & Laurikainen, E. 1994, ApJ, 428, 65
Henry, J. P., Soltan, A., Briel, U., & Gunn, J. E. 1982, ApJ, 262, 1
Hill, G. J., & Lilly, S. J. 1991, ApJ, 367, 1
Hodges, M. W., & Mutel, R. L. 1987, in Superluminal Radio Sources, edited by J. A. Zensus and T. J. Pearson (Cambridge University Press, Cambridge), p. 168
Hutchings, J. B. 1987, ApJ, 320, 122
Kerr, F. J. 1968 in Nebulae and Interstellar Matter, edited by B. M. Middlehurst and L. H. Aller (University of Chicago Press, Chicago), p. 575
Kriss, G. A., Cioffi, D. F., & Canizares, C. R. 1983, ApJ, 272, 439
Maloney, P. R., Begelman, M. C., & Rees, M. J. 1994, ApJ, 432, 606
Marziani, P., Sulentic, J. W., Calvani, M., Perez, E., Moles, M., & Penston, M. V. 1993, ApJ, 410, 56
Mirabel, I. F. 1989, ApJ, 340, L13
Mirabel, I. F., Sanders, D. B., & Kazes, I. 1989, ApJ, 340, L9
Morganti, R., Fanti, R., Gioia, I. M., Harris, D. E., Parma, P., & de Ruiter, H. 1988, A&A, 189, 11
Mulchaey, J. S., Davis, D. S., Mushotzky, R. F., & Burstein, D. 1995, ApJ (in press)
Napier, P. J., Thompson, A. R., & Ekers, R. D. 1983, Proc. IEEE, 71, 1295
O'Dea, C. P. 1990, MNRAS, 245, 20P
O'Dea, C. P., Baum, S. A., & Morris, G. B. 1990, A&AS, 82, 261
O'Dea, C. P., Baum, S. A., & Stanghellini, C. 1991, ApJ, 380, 66
O'Dea, C. P., Heckman, T. M., Baum, S. A., & Laurikainen, E. 1994, in Proceedings of the First Stromlo Symposium: The Physics of Active Galaxies, ASP Conf. Ser. Vol. 54, edited by G. V. Bicknell, M. A. Dopita, and P. J. Quinn (ASP, San Francisco), p. 209
Pearson, T. J., & Readhead, A. C. S. 1988, ApJ, 328, 114
Peterson, B. A., Savage, A., Jauncey, D. L., & Wright, A. E. 1982, ApJ, 260, L27
Pfeffermann, E., *et al.* 1987, in Soft X-ray Optics & Technology, edited by E.-E. Koch and G. Schmahl, Proc. SPIE 733 (SPIE, Bellingham), p. 519
Phillips, R. B., & Mutel, R. L. 1982, A&A, 106, 21.
Prestage, R. M., & Peacock, J. A. 1988, MNRAS, 230, 131
Raymond, J. C., & Smith, B. W. 1977, ApJS, 35, 419

Readhead, A. C. S., Taylor, G. B., Xu, W., Pearson, T. J., Wilkinson, P. N., & Polatidis, A. G. 1995, ApJ (in press)
Sanders, D. B., Soifer, B. T., Elias, J. H., Nuegebauer, G., & Matthews, K. 1988, ApJ, 328, L35
Sarazin, C. L. 1986. Rev. Mod. Phys., 58, 1
Shaw, M. A., Tzioumis, A. K., & Pedlar, A. 1992, MNRAS, 256, 6P
Sarazin, C. L. 1988, X-Ray Emission from Clusters of Galaxies (Cambridge University Press, Cambridge)
Scoville, N. Z., & Sanders, D. B. 1987, In Interstellar Processes, edited by D. Hollenbach and H. Thronson (Reidel, Dordrecht), p. 21
Smith, E. P., & Heckman, T. M. 1989, ApJ, 341, 658
Smith, E. P., O'Dea, C. P., & Baum, S. A. 1995, ApJ, 441, 113
Stanghellini, C., O'Dea, C. P., Baum, S. A., & Laurikainen, E. 1993, ApJS, 88, 1
Stanghellini, C., *et al.* 1995, in preparation
Stickel, M., & Kühr, H., A&AS, 105, 67
Trümper, J. 1983, Adv. Space. Res., 2, 24
Ulrich, M.-H. 1989, in BL Lac Objects, edited by L. Maraschi, T. Maccacaro, and M.-H. Ulrich (Springer, Berlin), p. 45
Verschuur, G. L. 1974, in Galactic and Extra-Galactic Astronomy, edited by G. L. Verschuur and K. I. Kellermann (Springer, New York), p. 27
Wade, R. A., Hoessel, J. G., Elias, H., & Huchra, J. P. 1979, PASP, 91, 35
West, M. J. 1994, MNRAS, 268, 79
Wilkinson, P. N., Booth, R. S., Cornwell, T. J., & Clark, R. R. 1984, Nature, 308, 619
Wilkinson, P. N., Polatidis, A. G., Readhead, A. C. S., Xu, W., & Pearson, T. J. 1994, ApJ, 432, L87
Worrall, D. M., & Birkinshaw, M. 1994, ApJ, 427, 134
Worrall, D. M., Birkinshaw, M., & Cameron, R. A. 1995, ApJ, 449 (in press)
Worrall, D. M., Lawrence, C. R., Pearson, T. J., & Readhead, A.C.S. 1994, ApJL, 420, L17
Worrall, D. M., *et al.* 1992, in Data Analysis in Astronomy IV, edited by V. Di Gesu *et al.* (Plenum, New York), p. 145
Yates, M. G., Miller, L., & Peacock, J. A. 1989, MNRAS, 240, 129
Young, J. S., & Scoville, N. Z. 1991, ARA&A, 29, 581
Zhang, Y. F., & Marscher, A. P. 1994, in Proceedings of the 1993 *ROSAT* Science Symposium, edited by E. Schlegel and R. Petre (American Institute of Physics, New York), p. 406
Zhang, Y. F., Marscher, A. P., Aller, H. D., Aller, M. F., Teräsranta, H., & Valtaoja, E. 1994, ApJ, 432, 91